

Anomaly Detection from Low-dimensional Latent Manifolds with Home Environmental Sensors

Francisco M Melgarejo-Meseguer, Andrés Lorenzo-Bleda, Sergio Eduardo-Abbenante, F-Javier Gimeno-Blanes, Estrella Everss-Villalba, Sergio Muñoz-Romero, José-Luis Rojo-Álvarez, *Senior Member, IEEE*, Rafael Maestre Ferriz

Abstract—Human Activity Recognition poses a significant challenge within Active and Assisted Living (AAL) systems, relying extensively on ubiquitous environmental sensor-based acquisition devices to detect user situations in their daily living. Environmental measurement systems deployed indoors yield multiparametric data in heterogeneous formats, which presents a challenge for developing Machine Learning-based AAL models. We hypothesized that anomaly detection algorithms could be effectively employed to create data-driven models for monitoring home environments and that the complex multiparametric indoor measurements can often be represented by a relatively small number of latent variables generated through Manifold Learning (MnL) techniques. We examined both linear (Principal Component Analysis) and non-linear (AutoEncoders) techniques for generating these latent spaces and the utility of core domain detection techniques for identifying anomalies within the resulting low-dimensional manifolds. We benchmarked this approach using three publicly available datasets (hh105, Aruba, and Tulum) and one proprietary dataset (Elioth) for home environmental monitoring. Our results demonstrated the following key findings: (a) Nonlinear manifold estimation techniques offer significant advantages in retrieving latent variables when compared to linear techniques; (b) The quality of the reconstruction of the original multidimensional recordings serves as an acceptable indicator of the quality of the generated latent spaces; (c) Domain detection identifies regions of normality consistent with typical individual activities in these spaces; And (d) the system effectively detects deviations from typical activity patterns and labels anomalies. This study lays the groundwork for further exploration of enhanced methods for extracting information from MnL data models and their application within the AAL and possibly other sectors.

Index Terms—Autoencoders, Deep Learning, Human Activity Recognition, Anomaly Detection, Sensors, Active and Assisted Living, Latent Spaces.

I. INTRODUCTION

AGEING POPULATION in developed countries is one of the biggest challenges for our society during the last decades. A moderate growing trend of the aged population (65 years and over) was identified between 1950 (11%) and 2000 (18%), but this trend will rise dramatically by 2050 when it reaches 38% [1]. The increasing number of elderly care services expends many social resources from national health care systems. One of the most known is the support of initiatives related to Active and Assisted Living purposes, with

the primary goal of providing necessary services for senior citizens at a manageable cost [2], through the deployment and use of technological solutions focused on promoting elderly independence and providing new intelligent functionalities for helping them on their daily living needs. It is feasible to come across research concerning Ambient Assisted Living (AAL), which involves using a platform that incorporates an array of sensors and devices to observe the health and welfare of senior citizens [3]. Furthermore, some undertakings strive to devise an all-inclusive remedy for the AAL of older people, which entails a platform that blends various sensors, devices, and services to furnish bespoke assistance to them [4]. Human Activity Recognition (HAR) plays a significant role in human-to-human interaction and interpersonal relations. The human ability to recognize another person's activities is one of the main subjects of study in the scientific areas of computer vision and machine learning (ML) [5]. The goal of HAR is to automatically detect and analyze human activities from the information acquired from sensors, e.g., a sequence of images, either captured by RGB cameras, range sensors, or other sensing modalities [6]. Current AAL systems often face the challenge of processing a wide variety of multiparametric data from environmental measurement systems: temperature, humidity, and light intensity by environmental sensors, while wearable sensors continuously measure respiration, pulse, and movement signals from gyroscopes and accelerometers to monitor daily activities such as sitting, walking, going upstairs and downstairs, standing, or resting [7], [8].

This diversity and density of measurements are often being tackled in terms of ML and Deep Learning (DL) methods nowadays, which often follow a classification problem statement regarding different activities to be recognized. Recent reviews on DL techniques for HAR with sensors suggest that efficient methods are emerging [9], [10]. However, interpretability is more complex in them. Another type of problem solved with data-based models in AAL is anomaly detection. Changes in typical patterns of daily activities are defined as anomalies, and data models aim to infer when a given pattern is notably different from the ones observed before. Linear dimensionality reduction techniques have been used in this setting, for instance, with conventional methods such as Principal Component Analysis (PCA) [11]. AutoEncoders (AE) architectures have been proposed [12] for anomaly detection in smart home systems, and they have given promising results. Interestingly, in this and other DL works, anomaly detection is often addressed in terms of the error reconstruction of the

FMMM, SMR, and JLRA are with Universidad Rey Juan Carlos, Madrid, Spain. FJGB y EEV are with Universidad Miguel Hernández de Elche, Spain. FJGB, SMR, and JLRA are with Dilemma Ltd startup, Fuenlabrada, Spain. ALB, SEA, and RMF are with CETEM, Murcia, Spain. *Corresponding author FMMM, email: francisco.melgarejo@urjc.es*

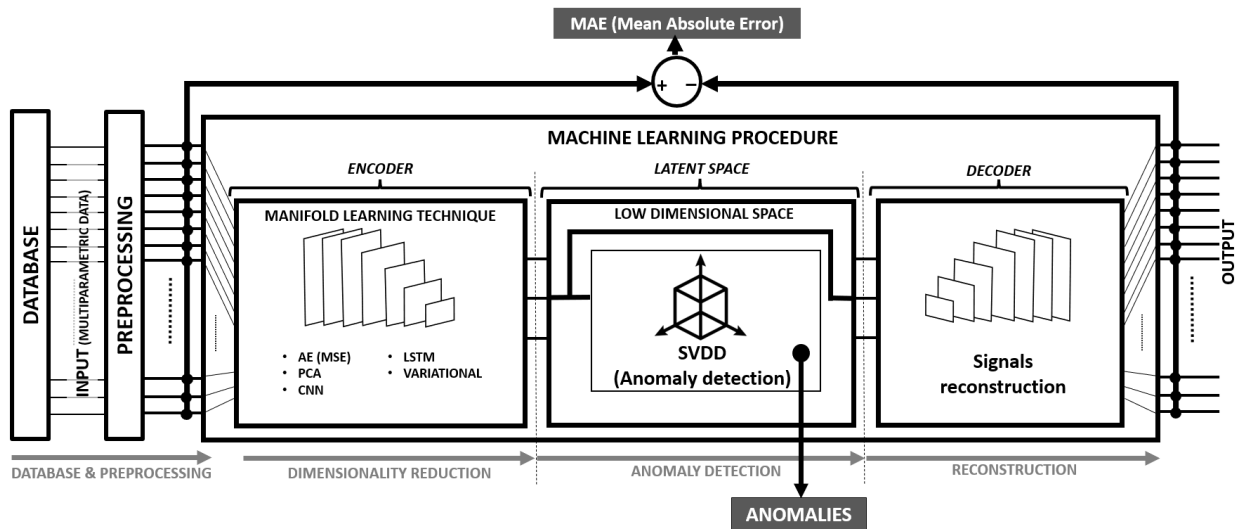


Fig. 1. The proposed system block diagram on the ML Procedure includes dimensionality reduction (encoder), anomaly detection (in the latent space), and reconstruction of the input (decoder). The machine learning core consists of two main components: the encoder, which maps the input into a low-dimensional latent space, and the decoder, which maps the small space into the reconstruction of the original input. Anomalies are assumed to be deviations of the mapping of an input vector from their usual manifold in the latent space.

input at their output. Still, again, the interpretability that could be achieved from the bottleneck of these structures needs to be explored. We can note here that AE can be seen as a Manifold Learning (MnL) method when we work only with the encoder component after training them. MnL methods are considered a subgroup of nonlinear dimensionality reduction procedures [13]. They are used assuming that high-dimensional data can be projected onto a low-dimensional latent space, whose variables represent the essential information of the original data set.

Whereas MnL techniques are often used for visualization purposes in ML and DL, anomaly detection algorithms could be used for creating models for home environmental monitoring, and multiparametric indoor measurement recordings could be represented by a moderate number of latent variables generated by MnL techniques. This way, sensor anomalies could be successfully detected to the security and functionality of the various sensors and devices. Therefore, we hypothesized that in-home sensor data and some algorithms would be able to capture subtle changes in usual patterns of daily activities that reflect early indicators of atypical situations, thus allowing generated alerts to be further scrutinized in AAL systems. For this aim, we implemented and benchmarked several anomaly detection algorithms based on low-dimensional representations of AAL recordings. We tested the different methods on several publicly available sensor HAR datasets (hh105, Aruba, and Tulum [14]) and on a home environmental setting with people in their living environments and the presence of integrated sensors at the so-called Elioth platform. Therefore, this work presents a novel system capable of detecting anomalies in daily living activities based on home sensor network registers.

II. METHODS

Our proposed system can be divided into three main parts: database processing, dimensionality reduction, and anomaly

detection (see Figure 1). The notation is as follows. We have an environment E for which a number of L measurements are monitored with time, this is,

$$m_l^E(t), l = 1, \dots, L \quad (1)$$

where m_l^E denotes the l^{th} signal in time taking place in environment E . Different sampling periods can be used for each signal (T_l) so that after digitizing and sending, we store the following digitized recordings:

$$m_l^E[n] = m_l(nT_l), n = 0, \dots, N_l - 1 \quad (2)$$

where $m_l^E[n]$ denotes the time-sampled version of the corresponding time signal, and $N_l - 1$ is the number of samples available in the digitized recording.

A. Databases and Preprocessing

We tested our method in four environments, three from publicly available repositories and one sustained by the research group at CETEM. Their characteristics are explained next.

Human Activity Recognition from Continuous Ambient Sensor Data (hh105) is a publicly accessible dataset available through the WSU CASAS repository [15]. This dataset covers five years, starting from June 2011 and ending in March 2017. To focus our study on the daily routines of House hh105, we specifically selected two months of data. From the extensive dataset, we narrowed our focus to data collected in the toilet, which includes sensors for light, temperature, and presence, as well as data from the kitchen, equipped with light and presence sensors. For a visual representation of the house layout and the positions of various sensors, see Figure 2.a.

Aruba is publicly available via the WSU CASAS repository [15]. This dataset covers a period of one year, extending from June 2016 to July 2017. Specifically, we have selected a two-month segment for an in-depth examination of the daily routines within House Aruba. This dataset has gained

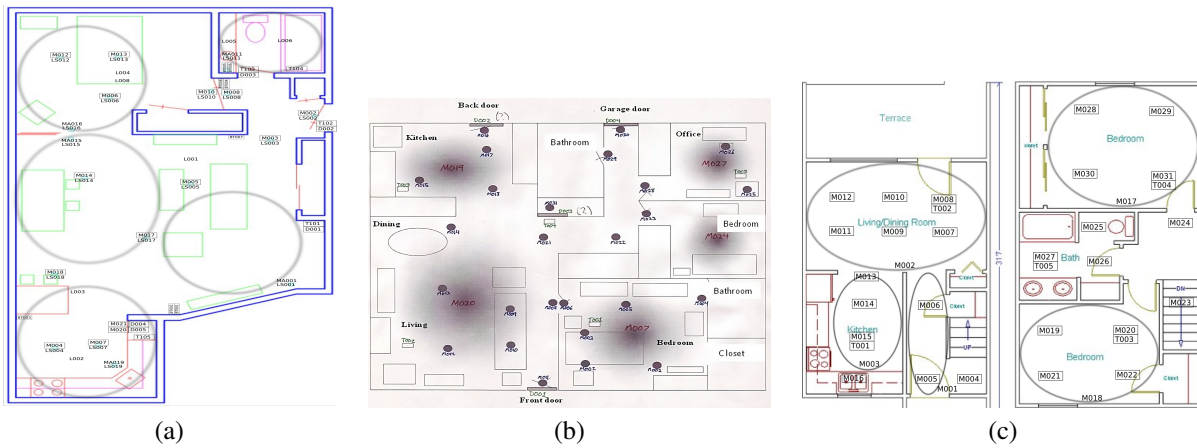


Fig. 2. House maps and their sensor positions for different datasets used. (a) shows the Human Activity Recognition from Continuous Ambient Sensor Data in the hh105 house, (b) shows the Aruba house, and (c) shows the Tulum house. Sensors labeled as MXXX refer to movement sensors, MAXXX refer to movement area sensors, and TXXX refer to temperature sensors. The other labels are not taken into account for this work.

recognition as one of the most frequently employed sensor datasets for assessing Human Activity Recognition (HAR) [14]. From this extensive dataset, we have focused on the data originating from the principal room, encompassing sensors monitoring temperature, movement, and presence. For a visual representation of the house layout and the various sensor placements, please consult Figure 2.b.

Tulum is a publicly accessible resource found within the WSU CASAS repository [15]. This dataset encompasses a timeframe of six months, ranging from September 2009 to March 2010. Specifically, we have selected a two-month segment to examine the daily routines within House Tulum closely. This dataset has garnered recognition as one of the most frequently utilized sensor data collections for assessing Human Activity Recognition (HAR) [14]. Within this extensive dataset, our focus is directed toward data originating from the principal room, where sensors are deployed to monitor temperature, movement, and presence. To gain insight into the layout of the house and the placement of various sensors, refer to Figure 2.c.

Elioth Environment. These databases have been selected to align with the main objective of the Elioth project, namely, the monitoring of older people to detect anomalies that can harm their health. For this reason, the selected databases collected data from homes where only one or two residents live. Elioth is a proprietary database collected during Elioth project. The data originates from 6 data acquisition devices (Elioth Sensor Devices) deployed in three homes (single-resident households). In each house, two data acquisition devices were set up, one in the living room and another in the main bedroom. However, our study exclusively utilizes the data collected from *House-1* during 36 consecutive days (ensuring a comprehensive and longitudinal dataset for our analysis).

In *House-1*, two data acquisition devices were deployed (*Sofa-1* and *Bed-1*). *Sofa-1* is located in the living room, precisely mounted on the wall next to the sofa and very close to a natural lighting window. *Bed-1* is in the house main bedroom, attached to the wall near the bed's headboard. There

are two main acquired data types:

- **Event Based-Data:** real-time sensor data associated explicitly with both occupancy and non-occupancy events detected on the couch and bed within the monitored environment.
- **Periodical Ambient Monitoring Based-Data:** real-time and periodic data from sensors related to ambient variables, including humidity, temperature, and lighting levels.

The Elioth Sensors Device enables seamless and non-intrusive monitoring of users in their home environment. One simply has to place the device in a fixed location and connect it to a power source and a WiFi data network (see Figure 3).

Preprocessing. The preprocessing stage is composed of two main parts. The first part involves extracting and curating different datasets, while the second part includes data normalization. Once the data are loaded, we need to apply resampling to equalize the different sampling frequencies of each sensor and dataset.

After conducting several tests, the data were reinterpolated to handle time resolution with one-day windows spaced every $T_s = 10$ minutes, resulting in a window size of 721 samples (144 samples per day, with each group representing 5 days). This yielded the following signal notation:

$$m_t^E[n] = m_i(nT_s), n = 0, \dots, N_t - 1 \quad (3)$$

Additionally, we included the timestamp in hours as a new signal, which can be denoted as

$$m_t^E[n] = n, n = n_0, \dots, N_t - 1 \quad (4)$$

where n_0 and $N_t - 1$ are reset and synchronized with zero at midnight. Note that this variable represents a relative time index that can be subsequently used as input for a daily temporal reference.

On the other hand, it was observed that the variables related to the presence or movement, when incorporated into the analysis directly, without transformation, did not expressively contribute to the final results in the presence of other variables or isolation. In this second case, it was observed that they

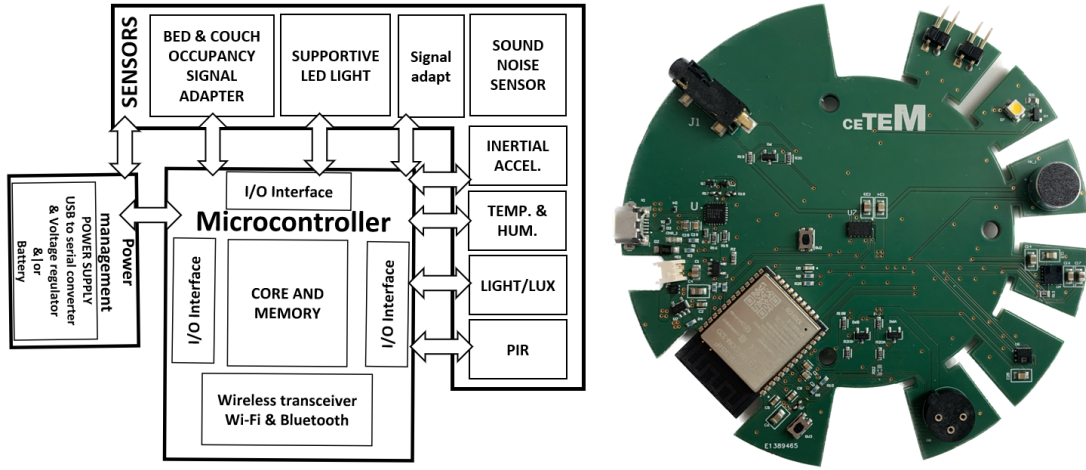


Fig. 3. Sensor node block diagram shows the components that collect, process, and transmit data from a physical environment. The Elioth device has Bluetooth and Wi-Fi capabilities for local configuration and data transmission to an external or cloud server. It includes: *two occupancy sensors* to detect the usage of a sofa or bed, which can be used to monitor resting and sleep patterns, *one accelerometer* to detect unusual device movements and impacts on the surface where it is installed, which can indicate possible falls, *one ambient noise sensor* to acquire anomalous sound levels, which can also be an indicator of possible falls or impacts and *one Presence InfraRed (PIR) motion detector* based on differences in heat emission, which is related to user's level of activity at home. Discrete and based event data, such as occupancy of the bed or sofa (0 for non-occupancy, 1 for occupancy), human presence (by the PIR sensor), unusual movements, impacts, or sound levels are acquired when a specific event happens as discrete variables (these events are recorded at specific moments, and do not change between timing moments). Additionally, to monitor the comfort level at home, Elioth includes a relative humidity (percentage), a temperature (in Celsius) sensor, and a lighting sensor (in Lux), which are continuous timing data acquired with a time interval of 15 minutes.

could not generate clear patterns, especially when they were consolidated into periods to make them compatible with the rest of the samples. This circumstance was produced by the intrinsic difference between the PIR state variables (an oscillating state signal that is difficult to consolidate into an equivalent evenly sampled time series), and actual continuous time series, such as temperature and humidity, are to be evaluated jointly. That is why part of the pre-processing included the transformation of these state variables into variables of temporary significance in order to be able to interact in a consolidated manner with the variables of continuous magnitude. To do so, we transformed each state variable into a set of time series by converting the state variable into these three synchronous variables: (1) A state variable that collected the state in the period as the majority state during it (Active/Inactive); (2) a second numerical variable that collects the number of status changes in the same period (Activations); And (3) a last variable that collects the duration of the active status. This led to a better characterization and compatibility for joint analysis without effective loss of information.

We denote globally with Φ_l the signal preprocessing operator, including the previous preprocessing stages on signals, in such a way that we denote

$$x_l^E[n] = \Phi_l\{m_l^E[n]\}, n = n_0, \dots, N_t - 1 \quad (5)$$

so that $x_l^E[n]$ denotes the discretized and preprocessed signal for the l^{th} sensor in environment E , and we can define similarly as $x_t^E[n] = \Phi_t\{m_t^E[n]\}$. The multivariable recording, denoted in matrix form as

$$\mathbf{X}^E[n] = [m_t^E[n]^T | m_1^E[n]^T | \dots | m_L^E[n]^T]^T \quad (6)$$

can be buffered in terms of the sliding window with size S samples, thus yielding the original data matrix,

$$\mathbf{X}^E[n] = \begin{bmatrix} x_t^E[n], & x_t^E[n-1], & \dots, & x_t^E[n-S+1] \\ x_1^E[n], & x_1^E[n-1], & \dots, & x_1^E[n-S+1] \\ \vdots & \vdots & \ddots & \vdots \\ x_L^E[n] & x_L^E[n-1], & \dots & x_L^E[n-S+1] \end{bmatrix}^T \quad (7)$$

and the complete data matrix is obtained as follows,

$$\mathbf{X} = [\mathbf{X}^E[1]^T | \dots | \mathbf{X}^E[N_t]^T]^T \quad (8)$$

In order to use a machine learning strategy for splitting the matrix data into train and test vectors, we choose a time instant n_{tr} to split the matrix into observed vectors so that

$$\mathbf{X}_{tr} = [\mathbf{X}^E[1]^T | \dots | \mathbf{X}^E[n_{tr}]^T]^T \quad (9)$$

are used as train vectors, and the others are used as test vectors. Note that an additional reshaping has to be done to convert the multiparametric temporal samples into a single vector, as usual in machine learning implementations, which is not included in this notation.

Finally, for the normalization stage, we propose three different scenarios. First, normalizing the data with respect to the absolute maximum of the signal values from the training set. Second, normalizing the data according to the z-score on the training set. And finally, not applying any normalization.

B. Dimensionality Reduction

Some AE, such as Naive (MSE), are neural networks trained to set a target equal to the input. They consist of two main components: the encoder, which maps the input into a small space called (latent space, initial compression of variables), and the decoder, which maps the small space

into the reconstruction of the original input. Although full recovery of the original signal will not be possible due to intermediate compression of the variables, by minimizing the difference between the original and final space, models defined in this way will preserve the essence of the data. They can generalize better on new samples and extend over a different or incremental sample space to perform full ML validation and testing processes [16]. A comparative methodology has been developed for several of these AE studies based on the results obtained from the different proposed techniques.

PCA is a linear multivariate statistical technique widely used as a dimension reduction technique for data compression or visualization. Analyzes a data set that represents observations described by several metric variables that are generally correlated with each other. Its goal is to represent this set of observed metric variables in terms of a smaller set of new orthogonal variables [17]. Detailed equations can be found in many works, and here we summarize the description [18]. This analysis, valid in many environments and data sets, cannot capture the nonlinear patterns often present in natural data. The representation of our data does not seem to be geometric and also presents a spatial dissociation between the training and test samples, so we use this technique to compare. MnL methods are considered a subgroup of nonlinear dimensionality reduction procedures [13] and are used under the assumption that high-dimensional data can be projected onto a manifold of low dimensions, representing the essential information of the original data set.

AE-based Manifolds. One of the most used manifold learning techniques is the AE architecture, which is a neural network compounded by three different parts, namely, the encoder, which applies a non-linear dimensionality reduction to input data \mathbf{x}_i , the code also called latent variables \mathbf{h}_i , which is the low dimensionality representation of input data, and the decoder, which perform a non-linear dimensionality augmentation of $\mathbf{h}(t)$ reaching the input space dimensionality $\hat{\mathbf{x}}_i$ [16]. From a structural point of view, the encoder and decoder nets are essentially the same. They may include zero or more hidden layers that are trained as classical artificial neural networks, but considering that the loss function intends to minimize the difference between input \mathbf{x}_i and output $\hat{\mathbf{x}}_i$.

Similarly to classical neural networks, the next equations describe the encoder block:

$$\mathbf{h}_i = \phi(\mathbf{W}_e \mathbf{x}_i + \mathbf{b}_e)$$

where $\mathbf{h}_i \in \mathbb{R}^d$ is the vector map in the latent space that corresponds to input $\mathbf{x}_i \in \mathbb{R}^D$, $\phi(\cdot)$ is a nonlinear transformation, \mathbf{W}_e is the weight matrix, and \mathbf{b}_e is the bias vector. Its corresponding decoder is also an affine mapping, given as

$$\hat{\mathbf{x}}_i = \varphi(\mathbf{W}_d \mathbf{h}_i + \mathbf{b}_d)$$

where $\varphi(\cdot)$ is another nonlinear transformation, \mathbf{W}_d is the weight matrix, and \mathbf{b}_d is the bias vector. We want to estimate the weights and biases \mathbf{W}_e , \mathbf{W}_d , \mathbf{b}_e , and \mathbf{b}_d , from a set of samples such that $\hat{\mathbf{x}}_i \approx \mathbf{x}_i$. Typical loss functions are the mean squared error and the cross-entropy metric.

Naive AE is the most direct approach, and it assumes the use of an input and output network consistent with a multilayer

neural network architecture that compresses the information at its intermediate point until reaching the desired dimensionality. In the second phase, the expansion occurs until the original space has a symmetrical structure compared to the first one. Use the MSE as a reflection of the quality of the analysis performed. *Convolutional Neural Network (CNN)* can consider the intrinsic temporal structure of the data with certain advantages over the conventional model [19], [20]. *Variational AE* can offer better performance due to its statistical foundation in the embedded space and the representation of the generated embeddings. *Long Short-Term Memory (LSTM)* is a type of recurrent neural network in which information can persist by introducing loops in the network diagram, which formalizes the existence of memory in the network and accumulates information from previous moments.

The encoder projection to low-dimensional latent space, called bottleneck, forces the AE to retain the essential information in the input data so that AE can be naturally seen as manifold estimators. Manifolds obtained from AE can be used on new test samples to support (and they often do) the use of other ML data models. Compared with PCA, the AE architecture provides us with nonlinear mappings for estimating the latent spaces, which, depending on the nature of the input data, can represent an advantage that should justify their use and the computational burden required by their training process.

C. Anomaly Detection

Identifying elements with different patterns outside the surface may be considered anomalies, as they have not been previously incorporated. There are several methods to detect anomalies, including machine learning (ML) and deep learning (DL), which have become increasingly popular [21], [22]. However, detecting anomalies in high-dimensional spaces and understanding the variables related to the anomaly can be challenging. A comprehensive review of detection techniques based on incoming or anomalous time series data can be found in [23].

The anomaly detection problem can be approached as complementary to the Domain Description (DD) problem. DD can be formulated as a one-class classifier, where an ML algorithm identifies the most common space region for a dataset and establishes a boundary to identify anomalous samples outside. Several algorithms can be used for DD, including the Support Vector DD (SVDD)[24], which is a kernel method that builds a boundary on a hypersphere mapped through kernel functions to an intermediate Reproducing Kernel Hilbert Space (RKHS). In this space, data can be adequately surrounded by a hypersphere corresponding to a nonlinear domain boundary [25].

The problem is to find the hypersphere with minimum volume in the RKHS that contains most of the mapped objects with radius $R > 0$ and center $\mathbf{a} \in \mathcal{H}$, given a dataset $\mathbf{x}_i \in \mathbb{R}^N$ belonging to a class of interest. To account for atypical values in the training set, slack variables $\xi_i \geq 0$ can be used. The

TABLE I
ARCHITECTURE MODEL WITH IMPROVED RESULTS FOR THE
EXPERIMENTS PERFORMED.

Choice	
Segmentation	30% training, 70% test
Time	yes
Windowing	24h
Normalization	Z-score
Layer and nodes	1[8]

problem can be formulated as

$$\min_{R, \mathbf{a}} \left\{ R^2 + C \sum_{i=1}^N \xi_i \right\} \quad (10)$$

subject to

$$\|\phi(\mathbf{x}_i) - \mathbf{a}\|^2 \leq R^2 + \xi_i \quad \forall i = 1, \dots, N \quad (11)$$

$$\xi_i \geq 0 \quad \forall i = 1, \dots, N \quad (12)$$

The trade-off between the hypersphere volume and the allowed errors is controlled by parameter C , while parameter $\nu = 1/(NC)$ is a rejection parameter that can be tuned [26]. The dual functional for this problem is a Quadratic Programming problem that gives Lagrange coefficients (α_i) corresponding to the constraints in Equation (11). When C is properly adjusted, many α_i are null, resulting in a sparse solution. Using the Lagrange multipliers obtained from the dual functional, we can calculate the distance of any point to the center in the RKHS, $R(\mathbf{x}_*)$, as per

$$R(\mathbf{x}_*) = K(\mathbf{x}_*, \mathbf{x}_*) - 2 \sum_{i=1}^N K(\mathbf{x}_i, \mathbf{x}_*) + \sum_{i,j=1}^N K(\mathbf{x}_i, \mathbf{x}_j) \quad (13)$$

This distance can be compared with the hyper-sphere radius R to determine if the input points are outside the domain. The equation calculates the distance by subtracting twice the sum of the kernel function evaluated at the input point and each training point from the kernel function evaluated at the input point itself and adding the sum of the kernel function evaluated at each pair of training points.

SVDD methods can be applied regardless of the data dimensionality. However, their primary interest in this work is their ability to identify the manifold structure in the low-dimensional latent space. This manifold structure can be represented and used to work with geometrical considerations on the manifold obtained from the input datasets.

D. Analysis and Visualization Code

Our customized software, a proprietary yet transparent tool, has been thoroughly validated for its efficacy in identifying normality patterns and anomalies across the hh105, Aruba, Tulum, and Elioth databases. This software enables us to:

- Independently select input variables for analysis, including temporary preprocessing.
- Utilize various analytical methods such as PCA, Naive AE, Variational AE, CNN, and LSTM.
- Configure the number of layers and nodes within each layer, allowing for exploring numerous configurations.

- Define a classification surface encompassing training data normality samples in the latent space, implicitly establishing a measure of normality represented as the distance to this surface (referred to as *score*).

Note that despite being a proprietary tool, the transparency and reproducibility of our results remain intact. The community has access to the code for various elements integrated into our software, ensuring the accessibility and verifiability of the techniques employed in the present work.

III. EXPERIMENTS AND RESULTS

The object and expected result of this task will be the identification of behavior patterns from the signals collected by the sensors that allow characterizing various situations of the daily reality of users at home. The proposed techniques will make it possible to analyze and, where appropriate, classify these situations as standard or be detected as anomalies. This second status classification may eventually allow experts to evaluate it for the corresponding intervention. Our results proved that: (1) The use of manifold nonlinear estimation techniques can provide significant advantages in the latent variables retrieved when compared with linear techniques; (2) The quality of the reconstruction of the original multidimensional recordings is an acceptable indicator of the quality of the generated latent spaces; (3) DD provides regions of normality consistent with representations of the usual activity of individuals in these spaces; (4) The system is capable of detecting deviations of the usual activity and label anomalies. The presented work paves the way toward exploring improved methods of retrieving information from MnL data models and their application in the AAL sector.

A. Latent Spaces

Some Elioth devices were installed in the homes of volunteer participants To carry out this project. A group of senior citizens was invited to recreate this kind of user's actual circumstances and patterns. The collected signals were processed using the previously described preprocessor and dimensionality reduction techniques. For the Elioth database, many tests and exploratory experiments were carried out to validate the results obtained in the exhaustive previous analysis on the Kyoto database and widely referenced in the literature. Alternative experiments were proposed based on different: (i) Time windows and significant overlaps for each sample; (ii) Preprocessing models and normalizations of the input magnitudes; (iii) Alternatives for incorporating different groups of variables in the analysis; (iv) Division of training and test samples; (v) Dimensionality reduction techniques; (vi) Figures of merit; (vii) Neurons in the intermediate layers for EAs; (viii) SVDD sizes.

Variables were evaluated both independently and in a different set of groups. Results showed that incorporating environmental variables, with or without the time variable, facilitated the cyclical characterization of the samples under analysis. On the contrary, the analysis of the state variables, or their derivatives, in isolation, even with the transformation practiced, did not facilitate the formulation of patterns in the

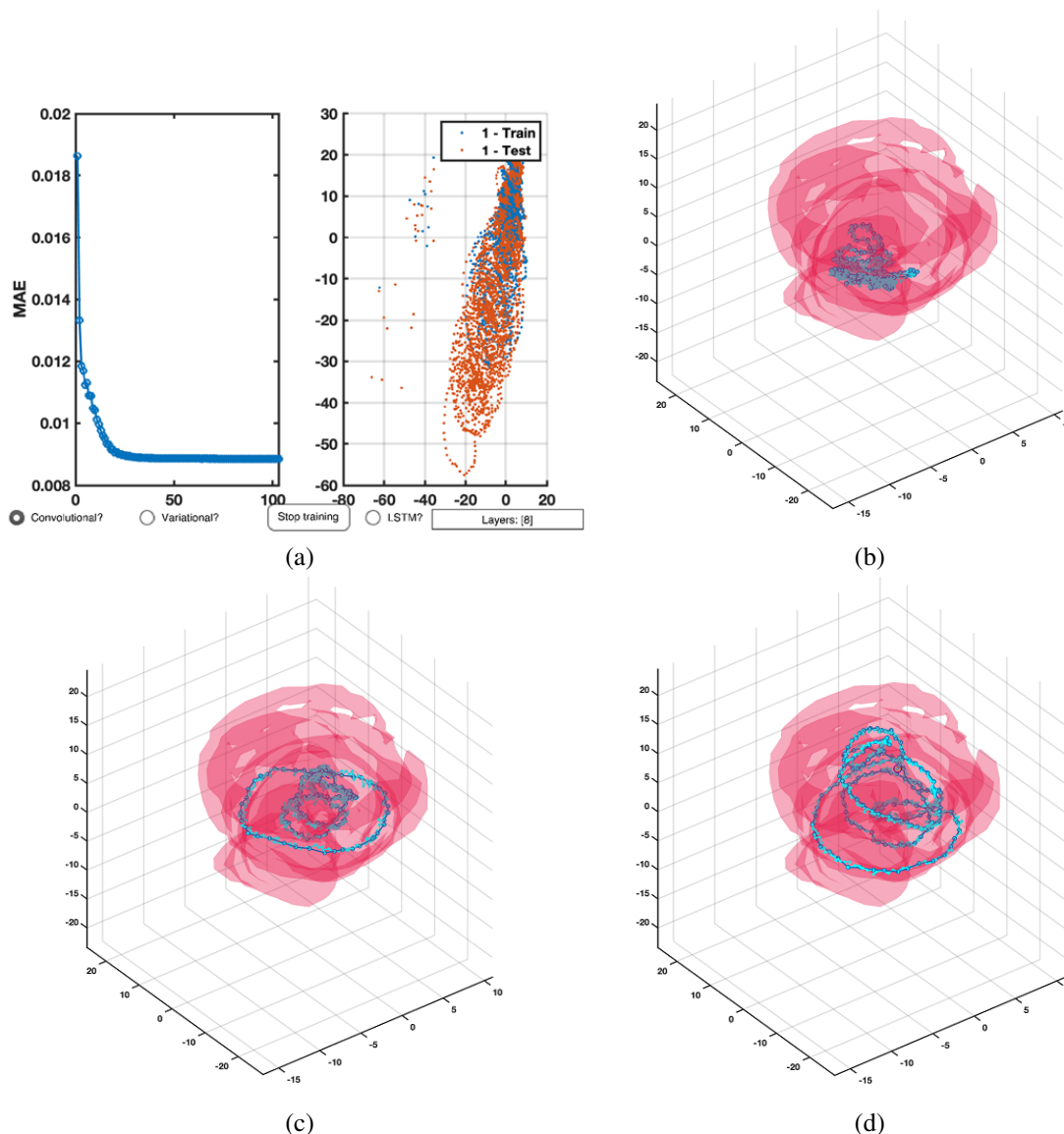


Fig. 4. Latent spaces calculated for the Toilet hh105 database: (a) the first panel shows the validation error obtained, and the second the latent space for the training set (blue), and test (orange) as they are computed by the proposed method. (b-d) shows different cases belonging to the test subset (in blue), and the pink volume represents the domain calculated over the training set.

TABLE II
MAE FOR EACH OF THE METHODS TESTED IN HH105-TOILET SENSORS.

Method	Illumination	Presence
PCA	0.0173	0.4042
Naive	0.0146	0.3094
CNN	0.0128	0.2576
Variational	0.0154	0.3369
LSTM	0.0166	0.3202

TABLE III
MAE FOR EACH OF THE METHODS TESTED IN HH105-ROOM SENSORS.

Method	Illumination	Presence
PCA	0.0346	0.4612
Naive	0.0215	0.3921
CNN	0.0187	0.3691
Variational	0.0246	0.3991
LSTM	0.0267	0.3761

latent space. The joint analysis of the state and environmental variables did not generate significant differences concerning the analysis of isolated environmental variables. It established an exciting result regarding the subtle contribution in the latent space generated by the state variables and their derivatives, slightly improving the figures of merit.

DL, ML, and AE have been analyzed to classify situations as everyday or as anomalies (and eventually allow their assess-

ment by experts for the intervention that could correspond). For this, a comparative methodology has been developed for the results obtained from the different techniques proposed for its analysis, whose characteristics have already been described: Naive, CNN, Variational, and LSTM.

The initial studies commenced with an analysis of the original Elioth and hh105 databases, during which decisions were made regarding parameter selection. These decisions

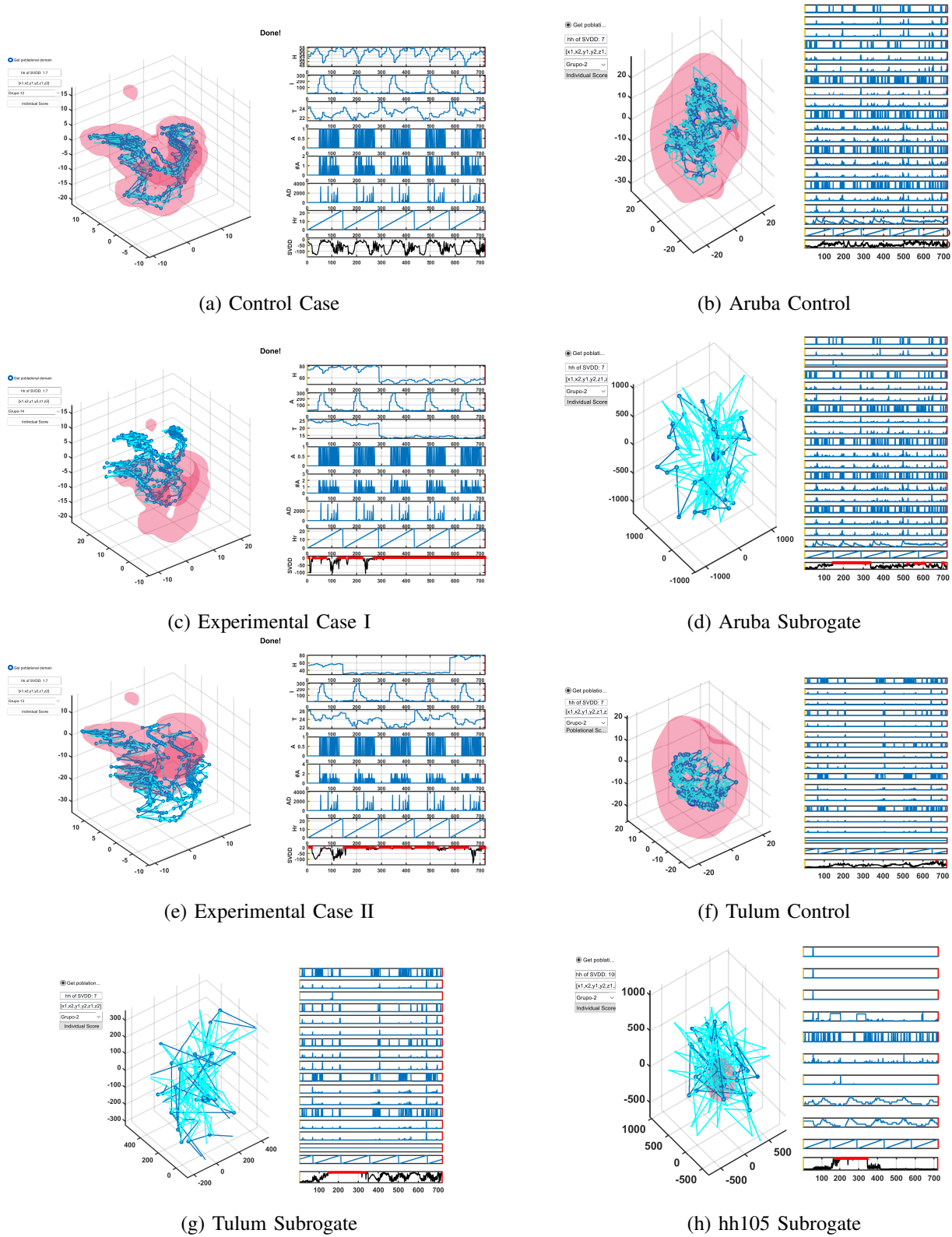


Fig. 5. Elioth, Aruba, Tulum, and hh105. In these illustrations, the left panel displays the embedded space represented in blue and the corresponding domain in pink, while the right panel showcases the signals used to compute this embedded space. See the text for a detailed explanation of the panels.

TABLE IV
MAE FOR EACH OF THE METHODS TESTED IN THIS WORK.

Method	Layers/Neurons	MAE
PCA	-	0,0089
Naive	[32,3]	0,0085
CNN	[8,3]	0,0085
Variational	[32,3]	0,0086
LSTM	[32,3]	0,0106

TABLE V
RECONSTRUCTION ERROR COMPUTED AS MAE FOR THREE DIFFERENT PUBLICLY USED DATASETS.

Dataset	MAE
hh105 Toilet	0,0085
Aruba Room	0.0029
Tulum Room	0.0099

encompassed various factors, including the proportion of cases allocated for training and testing, different sample window sizes, the consideration of variable normalization, and the determination of the appropriate number of layers and neurons for the aforementioned machine learning models (see Table I).

The circadian reality of the signals has shown the need to incorporate the time variable. Using widely overlapping daily time windows (24h) provided a cyclical perspective of the samples if they were represented sequentially. The incorporation of the normalization Z-max (division by the maximum) and Z-score (null mean and unit variance) improved the convergence and quality parameters, understood as errors of the selected figure of merit (MAE). The Z-score provided the best results when all the variables were incorporated jointly, and the Z-max was used in the individualized analysis of variables. The formulation of very complex architectures with high depth (many layers) and high dimensionality (many nodes per layer) did not show better results than the case of using a single layer with a reduced number of nodes. That is why a single layer with eight nodes has been proposed.

Given the results shown in Table I, tests were carried out again with the hh105 database in two rooms for each sensor in PCA and the different types of AE (Naive, CNN, Variational, LSTM) with different lighting, temperature, and presence sensors (see Tables II, III and IV. The analysis of the importance of each one of the sensors in the reconstruction of the test error (MAE) for each method showed that in the case of hh105-toilet sensors (Illumination (LS011/06) and Presence (MA011)) or hh105-room sensors (Illumination (LS010/12/13/16) and Presence (M10/12/13/16), those that provided the most information were the lighting sensors in all methods. CNN was the best, with the lowest reconstruction error (MAE).

Figure 4 shows the embedded space generated for all cases within the Toilet hh105 database. We can see the validation error obtained and the superimposed training and test sets in blue and orange, respectively. In (b-d), we can see the details of the embedded space for several cases of the training subset, with the spiral shape of the latent spaces notable, giving an idea of the quasi-periodicity of the analyzed data.

Once the previous experiment was conducted to tune the free parameters of the proposed method, namely the scheme

TABLE VI
DESCRIPTION OF ENVIRONMENTAL ANOMALIES.

Variable	Description
Humidity	Low (A1) reduction by 40% for 3 days (3cd)
	High (A2) increase by 40% for 3cd
Temperature	Low (A3) reduction by 40% for 3cd
	High (A4) increase by 40% for 3 cd
Lighting	Low (A5) not increase light in daylight periods
	High (A6) light is not dimmed at night for 3cd

TABLE VII
DESCRIPTION OF STATE ANOMALIES.

Lifestyle	Description
Sedentary (S): Daily (P1)	Lengthening of intervals of sitting in the chair
S: Nocturnal (P2)	Staying on the chair for hours
S: Afternoon (P3)	Staying on the couch before eating
Movement (M): At dawn (P4)	Sensor morning activation after hours before usually
M: At night (P5)	Gets up and sits down repeatedly
M: In regular hours (P6)	Unusual activity of the user (get up or sit down)

of dimensional reduction, the number of neurons, and the size of windows and overlaps, the method was tested on two different publicly available databases: the Aruba and Tulum datasets. Table V shows the performance of the selected method in terms of reconstruction error computed as MAE when compared with the hh105 dataset. As can be seen, the obtained MAE in both new datasets is close to that obtained using hh105, ensuring that the presented method is generalizable to different databases.

B. Anomaly Detection

As mentioned, in the traditional clustering approaches, DD can be done through support vectors (SV). Instead of directly kernelizing the metric or clustering algorithm, here we attempt to describe data distribution in feature spaces with a hypersphere of minimum volume enclosing all data points except outliers, resulting in a hypersurface in the original input space. This idea leads to several algorithms, such as the One-Class Support Vector Machine (OC-SVM) and the SVDD.

Once the normality space has been analyzed and considering the definition of anomaly described above, it is necessary to consider the possibility of characterizing the normality spaces on the original domains that allow the correct interpretability and validation of the results obtained. The detected anomaly and its corresponding signal from the original space were displayed to do this. The results obtained for the case of the Elioth database showed a broad normality regime with very little or no expression of anomalies. This reality is fully consistent with the behavior in the short-term test regime with healthy individuals, without behaviors of statistical significance throughout the records made. That is why, based on actual signals, a new set of records that simulate several eventualities was synthetically generated. These surrogated anomalies were classified according to whether the modified variable was an ambient or state variable. Here follows the description of the implemented anomalies (see Table VI and VII).

For the Elioth dataset, the complete study signal is built by incorporating the normal signals corresponding to a month and a half of recording (groups of signals from 1 to 12), and the concatenated surrogate signals with the anomalies A1 to A6 and P1 to P6 (groups 13 to 19). This signal is then introduced into the previously tuned algorithm to evaluate the normality spaces using the methodology mentioned earlier. In the case of hh105, Aruba, and Tulum, the experimental setup was slightly different. In these cases, we manually introduced anomalous P6 events on the 7th and 22nd day. The algorithm designed for this purpose allows us to display, across different groups of 5-day samples, both the generated population normality spaces and the score metrics (distance to the classification surface and domain description or SVDD). This metric (score) can be observed in the last graph in the right column of Fig. 5. The normality surface is observable in the three-dimensional graphs presented in the respective columns of the figures. It is worth noting that in certain instances, the surrogate anomaly exerts a significant influence on the calculated embedding, making it challenging to discern the normality surface. The various experiments allowed us to validate how increasing the width of the domain detector decreases the ability to detect anomalies in the test. Conversely, a width that is too narrow resulted in a high number of false positives. This fact emphasizes the importance of fine-tuning this method for correct detection.

In general, Fig. 5 represents together a set of representative plots for benchmarking purposes. Panels (a, c, and e) correspond to scenarios within the Elioth dataset: the Elioth control case, the Elioth surrogate case where humidity before sample 300 and temperature after sample 300 have been altered (Case I), and the Elioth surrogate case where humidity was altered between sample 150 and the end of the record. Panels (b and d) relate to scenarios within the Aruba dataset: the Aruba control case and the Aruba surrogate case, where the first motion sensor was altered around sample 144. Panels (f and g) correspond to scenarios within the Tulum dataset: the Tulum control case and the Tulum surrogate case, where the first motion sensor was altered around sample 144. Finally, Panel (h) pertains to a scenario within the hh105 dataset: the hh105 toilet surrogate case, where the first motion sensor was altered around sample 144. In the case of the Elioth dataset, the y-axis on the signal panel represents various parameters, including humidity (H), illumination (I), temperature (T), couch occupancy sensor state (A), count of couch occupancy sensor activations over a period (#A), couch occupancy sensor activation duration (DA), hour (Hr), and SVDD value (SVDD). For the other datasets, the signal panel y-axis corresponds to different sensor signals as specified in each dataset sensor list, along with the hour and the SVDD value.

The results showed how with the CNN method, it was possible to conveniently detect a large part of the anomalies through the red crosses (red x), as can be seen in Figure 5 (c), (d), (e), (g), and (h). In the same way, it can be observed that the samples corresponding to the normality space are included within the surface of the SVDD. In greater detail, after adjusting the parameters as previously indicated and appropriately setting the SVDD width, the proposed algo-

rithm accurately detects all environmental anomalies within the Elioth dataset. However, it does not effectively identify anomalies associated with state variables in this particular dataset. In contrast, the algorithm successfully detects state variable surrogations in the Aruba, Tulum, and hh105 datasets. This success can be attributed to the fact that these datasets primarily consist of state variables, which exert a strong influence on the generated embedding. Their anomalies were exceptionally detected during the synthesized anomalies for this last set of variables. This result is consistent with the exploratory analysis in the design phase, which suggested a limited participation of the state variables in the generated model.

IV. DISCUSSION

Our presented work proved that MnL estimation techniques could provide significant advantages in the latent variables retrieved compared to linear techniques. The reconstruction of the original multidimensional recordings tends to preserve the essence of the data, and DD provides regions of normality consistent with representations of users' daily activity in these spaces. The proposed system can detect deviations from the usual routine and classify them as anomalies.

Similarities between the analyses of the hh105, Aruba, and Tulum public databases and results obtained for the case of Elioth validate the methods used in this analysis. Our methods based on DL, moderate complexity (AE of minimum MSE), offer better compactness of the natural embeddings extracted from the data than multivariate methods classics like PCA.

Many methods have been applied to detect anomalies, and more recently, ML [21] and DL [22] are widely used in this context. The application of MnL techniques in the field of AAL, specifically for HAR, has posed a research challenge due to the diversity and nature of raw data. We conducted an exhaustive analysis and comparative methodology of complex latent spaces obtained from different MnL techniques. As mentioned earlier, multiparametric indoor sensor anomalies could be represented by a moderate number of latent variables generated by MnL techniques. Our algorithms can capture subtle changes in the usual patterns of daily activities, reflecting early indicators of atypical situations. Both LSTM and SVM demonstrated good accuracy in routine activities captured with gyroscopes and accelerometers in the aged population ([8], [7]). CNN provided the best results compared to other invertible methods. In other elaborate approaches [27], entropy measurements were employed. They detected anomalies with real data of daily activities carried out by elderly people in residences, distinguishing them from those carried out by staff or visitors' relatives.

The use of other types of contractive MnL algorithms, such as Uniform Manifold Approximation and Projection (UMAP) [28] could yield relevant advantages, as far as they work on the estimated topology of the input space to map it into low-dimensional latent spaces efficiently. UMAP has been conveniently implemented and analyzed during the analysis process. The non-existence of an inversion technique to the reconstructed space implemented in the platforms used in this

work has not allowed its characterization based on the figures of merit used and, therefore, was discarded as a utility model.

Some studies [29] have proposed using ML architectures like LSTM, CNN, or its combination (ConvLSTM) and concluded that multi-task learning effectively assesses the fall risk of older adults from accelerometer sensor data. Meanwhile, other research groups [30] have used SVM to recognize six ambulation activities with smart insoles. The inertial sensors were shown to be reliable for the recognition of dynamic activities. In contrast, pressure sensors worked better for stationary activities, and the highest accuracy was achieved by combining both types of sensors. New ML algorithms have been proposed and used to classify older adults at low or high risk of falling using inertial sensor data collected from a smartphone, and they worked better than standard ML techniques [31]. This group [14] classifies the techniques that generate better results in sensor datasets, and Recurrent Neural Networks considerably improve hit rates. A review of Tiny ML with novel wearable systems incorporating micro-controller units for monitoring, p.e., elderly fall detection, can provide several advantages over cloud computing [32].

SVDD-type techniques in the latent space on surrogated real signals with environmental anomalies were adequate for detecting anomalies with the selected optimum settings. On the contrary, the limited contribution of individual anomalies has shown the need to broaden the analysis, particularizing these separately from the environment and including the need to establish new signal formulation models and labeling that improve the detection capabilities of the techniques designed here.

With latent variables, Murase et al. [33] propose a generator of anomalous variables to train an anomaly detector that makes differences between atypical/normal variables. Jiang [34] proposes a novel mechanism to learn the temporal patterns of event sequences of common daily activities. Delay-caused anomalies are detected by comparing the sequence with the learned patterns and achieving high accuracies for daily activities like using the toilet. In [35], an approach for identifying the sources of abnormalities in human activities of daily living was successfully proposed with OC-SVM. A systematic literature review of randomized controlled trials [36], studies with assistive technologies showed positive results in well-functioning but not in frail older adults, suggesting that this is still an active research field with space for improvement. Our system can detect different anomalies in the daily living activities of elderly users based on sensor networks at home, and the ML algorithms proposed can detect potential risks for the user, including alertness levels of anomalies.

Several limitations and challenges remain. The definition of *anomalous behavior* has been done here from a DD viewpoint on a window of multiparametric measurements projected onto a low-dimensional latent space. It is evident that some anomalous behavior repeated with time can become as usual for the system, as far as it will consist of a sub-cloud of points in the overall latent space. Therefore, the machine learning definition of anomaly should be worked for each specific application in conjunction with the risks that could be established *a priori* or as essential, if this is possible. Similar considerations can

be made for establishing the statistical description and merit figures for detection (false positives, false negatives), which, in general, should be dependent on the system to be implemented. The performance will be initially tied to the adequate choice of the domain bandwidth in the DD problem, but refinements on temporal observation windows can be readily established according to the nature and critical requirements of each practical application.

In future works, we want to deepen the study of anomalies, which are formally very similar to other configurations of normality, if attention is paid to the temporary configuration of other instants. For this reason, we propose an improvement by studying new schemes for classifying input signals and pre-labeling that facilitate powerful descriptions of the posterior latent space by incorporating such input information. In addition, establishing frequencies of different sampling, especially on presence signals, could offer new analysis frameworks. It is proposed to carry out superior analyses in how much sampling frequency, as well as evaluating extending the sampling windows temporal analyses to sections of weeks, months, or years so that they can obtain patterns related to weekly cycle behaviors or cycle seasonality that could help to classify the events better.

The proposed framework can be extended to other types of scenarios, such as smart factories or the internet of vehicles, in which some studies [37], [38] have demonstrated the utility of SVDD as an anomaly detector. The presented model can offer a novel approach to these problems by analyzing the manifold and understanding the strength of each variable in the final decision. In this way, our processing can help enhance the interpretability of the model by inspecting the shape of the manifold created, allowing us to select the number and type of sensors that provide the best anomaly detection rate with the fewest sensors.

V. CONCLUSIONS

In this study, we have demonstrated the potential benefits of employing manifold nonlinear estimation techniques over traditional linear approaches in home monitoring environments. Our results indicate that these techniques can yield enhanced latent variable representations. Moreover, the quality of multidimensional recording reconstruction is a reliable indicator of the latent-space quality. Through domain detection, we have successfully identified regions of normality aligned with typical individual activities within these spaces. This system capacity to detect deviations from routine behavior and classify anomalies opens promising avenues for applications in the AAL sector. Our work lays the foundation for further exploration and refinement of information retrieval methods from Manifold Nonlinear Learning data models in this domain and probably in others, such as Industrial IoT.

In conclusion, the presented results underscore the significance of non-linear manifold estimation in IoT data analysis, particularly for AAL applications. The findings here affirm the value of focusing on the quality of latent spaces and their relationship to the reconstruction of original multidimensional recordings. This approach to domain detection

has demonstrated its practical utility in identifying normal activity patterns within these spaces and detecting anomalies. We encourage continued research into MnL data models, spurring advancements in data analysis methodologies and their meaningful utilization in the context of improving the quality of life and healthcare in AAL systems.

ACKNOWLEDGMENTS

This work was partially supported by Research Projects BigTheory (PID2019-104356RB-C41), HESTIA (2022-REGING-92049), and Intrinsic (PID2022-140786NB-C31) from Spanish Government. Research partially funded by the Autonomous Community of Madrid (ELLIS Unit Madrid).

REFERENCES

- [1] E. Rudnicka et al. The world health organization (who) approach to healthy ageing. *Maturitas*, 139:6–11, 2020.
- [2] A.-L. Bleda et al. Enabling heart self-monitoring for all and for aal—portable device within a complete telemedicine system. *Sensors*, 19(18):3969, 2019.
- [3] M. Arend et al. *Active ageing initiatives of older people in civil society: deliverable D5 and WP5*. Interdisciplinary Centre for Comparative Research in the Social Sciences (ICCR), 2005.
- [4] A. Astell et al. Inlife - independent living support functions for the elderly : technology and pilot overview, 2018.
- [5] M. Vrigkas et al. A review of human activity recognition methods. *Frontiers in Robotics and AI*, 2, 2015.
- [6] Aggarwal. Human activity recognition from 3d data: A review. *Pattern Recognition Letters*, 48:70–80, 2014.
- [7] E. Ramanujam et al. Human activity recognition with smartphone and wearable sensors using deep learning techniques: A review. *IEEE Sensors Journal*, 21(12):13029–13040, 2021.
- [8] A. Hayat et al. Human activity recognition for elderly people using machine and deep learning approaches. *Information (Switzerland)*, 13, 05 2022.
- [9] L. Dang et al. Sensor-based and vision-based human activity recognition: A comprehensive survey. *Pattern Recognition*, 108:107561, 2020.
- [10] K. Chen et al. Deep learning for sensor-based human activity recognition: Overview, challenges, and opportunities. *ACM Computing Surveys*, 54:1–40, 05 2021.
- [11] L. Van Der Maaten et al. Dimensionality reduction: a comparative review. *J Mach Learn Res*, 10:66–71, 2007.
- [12] T. Cultice et al. Smart home sensor anomaly detection using convolutional autoencoder neural network. In *IEEE International Symposium on Smart Electronic Systems (iSES) (Formerly iNiS)*, pp. 67–70, 2020.
- [13] J. A. Lee and M. Verleysen. *Nonlinear dimensionality reduction*. Springer Science & Business Media, 2007.
- [14] E. De la Hoz et al. Sensor-based datasets for human activity recognition – a systematic review of literature. *IEEE Access*, PP:1–1, 10 2018.
- [15] W. S. University. CASAS smart home data sets. <https://casas.wsu.edu/datasets/>. [Accessed September-2022].
- [16] P. Baldi. Autoencoders, unsupervised learning, and deep architectures. In *Proceedings of ICML workshop on unsupervised and transfer learning*, pp. 37–49, 2012.
- [17] H. Abdi and L. Williams. Principal component analysis. *WIREs Computational Statistics*, 2(4):433–459, 2010.
- [18] L. Bote-Curiel et al. Text analytics and mixed feature extraction in ovarian cancer clinical and genetic data. *IEEE Access*, 9:58034–58051, 2021.
- [19] A. Ghosh et al. *Fundamental Concepts of Convolutional Neural Network*, pp. 519–567. 01 2020.
- [20] I. Khan et al. Human activity recognition via hybrid deep learning based model. *Sensors*, 22(1):323, 2022.
- [21] A. B. Nassif et al. Machine learning for anomaly detection: A systematic review. *IEEE Access*, 9:78658–78700, 2021.
- [22] L. Ruff et al. A unifying review of deep and shallow anomaly detection. *Proceedings of the IEEE*, 109(5):756–795, 2021.
- [23] A. Blázquez-García et al. A review on outlier/anomaly detection in time series data. *ACM Comput. Surv.*, 54(3), apr 2020.
- [24] M. Kim et al. Active anomaly detection based on deep one-class classification. *Pattern Recognition Letters*, 167:18–24, 2023.
- [25] D. Tax and R. P. W. Duin. Support vector domain description. *Pattern Recognition Letters*, 20:1191–1199, 1999.
- [26] B. Schölkopf et al. Input space versus feature space in kernel-based methods. *IEEE Transactions on Neural Networks*, 10(5):1000–1017, 1999.
- [27] A. Howedi et al. An entropy-based approach for anomaly detection in activities of daily living in the presence of a visitor. *Entropy*, 22(8), 2020.
- [28] L. McInnes et al. Umap: Uniform manifold approximation and projection. *Journal of Open Source Software*, 3(29):861, 2018.
- [29] A. Nait et al. Deep learning to predict falls in older adults based on daily-life trunk accelerometry. *Sensors*, 18(5):1654, 2018.
- [30] Z. H. dArco L, Wang H. Assessing impact of sensors and feature selection in smart-sole-based human activity recognition. *Methods and Protocols*, 5(3):45, 2022.
- [31] M. Martínez and P. De Leon. Falls risk classification of older adults using deep neural networks and transfer learning. *IEEE J Biomed Health Inform.*, 24(1):144–150, 2020.
- [32] M. S. Diab and E. Rodriguez-Villegas. Embedded machine learning using microcontrollers in wearable and ambulatory systems for health and care applications: A review. *IEEE Access*, 10:98450–98474, 2022.
- [33] H. Murase and K. Fukumizu. Algan: Anomaly detection by generating pseudo anomalous data via latent variables. *IEEE Access*, 10:44259–44270, 2022.
- [34] C. Jiang et al. Effective anomaly detection in smart home by integrating event time intervals. *arXiv*, 2022.
- [35] S. Yahaya et al. Detecting anomaly and its sources in activities of daily living. *SN COMPUT. SCI.*, 2(1):14, 2021.
- [36] F. ML et al. The effectiveness of assistive technologies for older adults and the influence of frailty: Systematic literature review of randomized controlled trials. *JMIR Aging*, 5(2):e31916, 2022.
- [37] E. Gyamfi and A. D. Jurcut. Novel online network intrusion detection system for industrial IoT based on OI-SVDD and AS-ELM. *IEEE Internet of Things Journal*, 10(5):3827–3839, March 2023.
- [38] X. Li et al. CAN bus messages abnormal detection using improved SVDD in internet of vehicles. *IEEE Internet of Things Journal*, 9(5):3359–3371, March 2022.